Visible Light-Promoted Aryl Azoline Formation over Mesoporous Organosilica as Heterogeneous Photocatalyst

Wenxin Wei,[a] Run Li,[a] Niklas Huber,[a] Gönül Kizilsavas,[a] Calum T. J. Ferguson,[a] Katharina Landfester,[a] and Kai A. I. Zhang*[a, b]

N-heterocyclic compounds demonstrate wide applications ranging from natural compound production to coordination chemistry. Usually, the synthesis of N-heterocyclic compounds is conducted under thermal conditions, mostly by Lewis acids or metal-containing compounds as molecular catalysts. Here, we report a photocatalytic route for aryl azoline formation by mesoporous organosilica as visible light-active and heterogeneous photocatalyst. Via formation of aromatic aldehydes with various amines, 2-phenyl-2-imidazoline, 2-phenyl-2-oxazoline, 2-phenyl-2-thiazoline and their derivatives could be formed with high conversion and selectivity. Additionally, the organosilica photocatalyst showed high stability and reusability.

N-heterocyclic compounds are widely used as important basic structure for pharmaceuticals, agrochemicals or ligands in organometallic chemistry.[1] Among the vast number of *N*-heterocycles, 2-imidazolines, 2-oxazolines, and 2-thiazolines have received most attention as ubiquitous building blocks in biologically active natural products, drugs and enzyme inhibitors etc.[2] Until now, different preparative strategies have been developed to synthesize azoline derivatives.[3] Conventionally, the synthesis for *N*-heterocycles is conducted under thermal conditions, in which precisely designed catalysts such as Lewis acids[4] or transition metals are used.[5] Recently, more environmentally benign and milder reaction conditions involving photocatalysts has been reported.[6] Most of the used photocatalyst are of homogenous nature. Heterogeneous systems, which combine the advantages of photocatalysis and reusable heterogeneous catalyst, have barely been applied for the synthesis of *N*-heterocycles so far. Further studies in this field are highly desired.

Recently, visible light-active, porous organic and metal-free materials have been employed as photocatalysts in a variety of photoredox applications. Among them, covalent organic frameworks (COFs),[7] carbon nitride[8] and conjugated microporous polymers (CMPs)[9] have been developed for visible light-driven redox reactions such as water splitting, CO_2 reduction,[10] biosensing[11] and wastewater treatment[12] etc. These emerging photocatalysts have demonstrated advantages as low toxicity, low cost, stability and reusability. Taking advantage of the well-designed porous structure, the photocatalysts can be further endowed with high specific surface area with accessible active sites and further facilitating photocatalytic reactions with enhanced efficiency.[13] The diffusion of substrate molecules during the catalytic process into the micropores and therefore efficient contact to the active sites are limited.[14] To overcome this challenge, synthesis of heterogeneous photocatalysts with larger pores, in particular, mesoporous has been a focus for the chemists.

Mesoporous organosilica, with their throughout porous structure in the meso range, designable organic content and robust nature, could offer a promising platform for photocatalytic applications.[15] A well-designed morphology allows reagent molecules to easily diffuse into the mesopores and therefore the active catalytic centers within the photocatalysts.[16] Recent studies involving mesoporous silica-based materials have showed rather grafting methods for catalyst design.[17] Achieving high catalyst loading onto mesoporous silica is indeed challenging.[18] Light-driven organic redox reactions have been barely reported. It is indeed highly desired to develop mesoporous organosilica as efficient heterogeneous photocatalysts with high effective catalyst content and accessible pore structure for organic photoredox reactions. Herein, we report the design and synthesis of mesoporous organosilica with integrated 4,7-diphenylbenzothiadiazole (BTPh$_2$) units as efficient photocatalyst for the photocatalytic formation of *N*-heterocycles (Scheme 1). The content of the effective photocatalytic moieties within the organosilica network was controllable and their structure is easily designable. The organosilica showed a pore size of about 5.7 nm. Via formation of aromatic aldehydes with various diamines, 2-phenyl-2-imidazoline, 2-phenyl-2-oxazolines, 2-phenyl-2-thiazolines and their derivatives could be formed over the mesoporous organosilica as heterogeneous photocatalyst with high conversion and selectivity.

The synthesis details are described in the Supporting Information (SI). 1,4-bromophenyltriethoxysilane (BPTS) was chosen as the monomers for the synthesis of the backbone

[a] W. Wei, Dr. R. Li, N. Huber, Dr. G. Kizilsavas, Dr. C. T. J. Ferguson, Prof. K. Landfester, Prof. K. A. I. Zhang
Max Planck Institute for Polymer Research
55128 Mainz (Germany)
E-mail: kai.zhang@mpip-mainz.mpg.de
[b] Prof. K. A. I. Zhang
Department of Materials Science
Fudan University
Shanghai 200433 (P. R. China)
E-mail: kai_zhang@fudan.edu.cn

ChemCatChem

Communications
doi.org/10.1002/cctc.202002038

**Chemistry
Europe**
European Chemical
Societies Publishing

Scheme 1. Illustration of the design concept of the photocatalytic mesoporous organosilica and their application in aryl azoline formation via addition of aryl aldehydes and amine derivatives.

precursor MOS—Br. The photoactive diphenyl benzothiadiazole (BTPh$_2$) units were then formed via successive coupling methods, obtaining the final organosilica MOS—BT.

Scanning electron microscopy (SEM) and transmission electron microscopy (TEM) images showed a fused particle-like morphology of the organosilica (Figure 1a). TEM energy dispersive X-ray spectroscopy (TEM-EDX) of MOS—Br and MOS—BT revealed the successful conversion of the bromide groups on MOS—Br, proving the chemical composition of MOS—BT (Figure S1 in SI). Fourier transform infrared (FTIR) spectroscopy (Figure 1b) revealed recognizable signals at 1348, 1377, 1567 and 1577 cm^{-1}, which are the typical characteristics for C=N and N—S stretching modes in benzothiadiazole units. The strong and wide absorption signals at 1095 cm^{-1} can be assigned to Si—O—Si antisymmetric stretching vibration. The Brunauer-Emmett-Teller (BET) surface area of MOS—BT was determined to be 339 m^2/g, with pore diameter of ca. 5.7 nm (Figure S2 in SI).
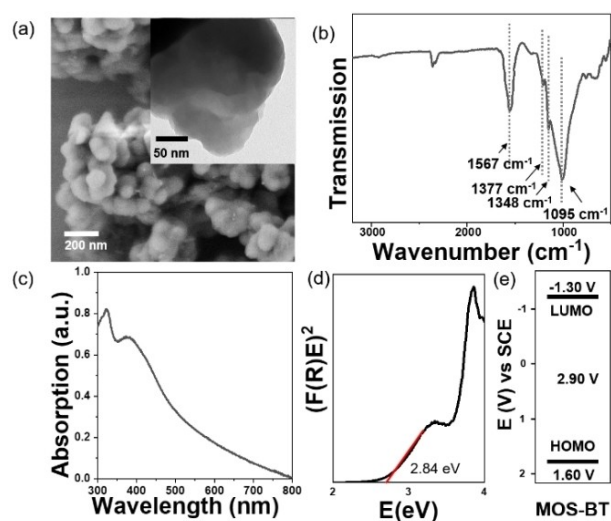
Figure 1. (a) SEM and TEM (insert) images, (b) FTIR, (c) UV/vis DR spectra, (d) Kubelka-Munk plot and (e) HOMO and LUMO band positions of MOS—BT.
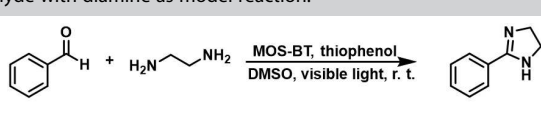
UV/vis diffuse reflectance spectrum (DRS) of MOS—BT (Figure 1c) revealed a broad absorption range until 800 nm. The absorption maximum at 395 nm can be assigned to that of the BTPh$_2$ unit. Photoluminescence spectrum showed a range between 425 nm and 700 nm with a maximum at 521 nm, which is similar to that of the BTPh$_2$ unit (Figure S3 in SI).[19] The slightly red shift of MOS—BT compared to the single BTPh$_2$ could be attributed to the hyper conjugation effect of the photoactive unit in MOS—BT. The optical properties of MOS—BT of emission and absorption behaviors are similar to those of *fac*-[Ir(ppy)$_3$], a well-established molecular transition metal photocatalyst.[20]

The optical band gap of 2.84 eV for MOS—BT could be derived from the Kubelka-Munk-function (Figure 1d). Cyclic voltammetry measurements indicated that the lowest unoccupied molecular orbital (LUMO) position of MOS—BT was at −1.30 V vs SCE (Figure S5 in SI). And the highest occupied molecular orbital (HOMO) position at 1.60 V vs SCE (Figure 1e). The HOMO and LUMO levels of MOS—BT matched the energy positions of BTPh$_2$. Theoretical calculations for the repeating unit (O—Si—Ph—BT—Ph) using density functional theory (DFT) on rB3PW91/6-311+g(d,p) level (Figure S4 in SI) revealed that the electron densities on HOMO and LUMO are mainly located on the BTPh$_2$ unit, indicating that the electronic structure is determined by the donor-acceptor (D—A)-type unit BTPh$_2$. Under nitrogen atmosphere, MOS—BT could remain intact up to 400 °C as revealed by thermogravimetric analysis (TGA) (see Figure S6 in SI). Inductively coupled plasma spectrometry (ICP) revealed the content of Pd residue below 0.5 ppm (Figure S7 in SI).

To investigate the photocatalytic activity of MOS—BT, the aryl azoline formation was chosen as model reaction for the photocatalytic formation of 2-phenyl-2-imidazoline. As listed in Table 1, the use of organosilica led to successful formation of phenyl azoline with selectivity higher than 95%, with MOS—BT being the most effective catalyst for a reaction conversion of 85% (entry 1). The molecular unit BTPh$_2$ used as homogeneous photocatalyst (applied with a similar loading) showed a full conversion of the 2-phenyl-2-imidazoline formation. MOS—BT showed a similar efficiency to its small molecular analogue. This indicates the good accessibility of the photocatalytically active moieties and diffusion of reactants throughout the pores in MOS—BT. Control experiments conducted in dark (entry 3), or without using MOS—BT as photocatalyst led only to trace conversion, demonstrating the essential roles of light and photocatalyst. The same phenomenon was cognized by excluding thiophenol and oxygen from the reaction atmosphere (entries 4, 5 in Table 1). Furthermore, various solvents (entries 6, 7 and 8 in Table 1) were investigated. After comparing, the reaction containing dimethyl sulfoxide as solvent (entry 1 in Table 1) was found with highest conversion.

Electron and hole scavengers were then included to exposure the mechanistic insight and the specific roles of the photogenerated electron/hole pair during the addition process. By adding CuCl$_2$ as an electron scavenger, a reduced conversion was observed (entry 9). With the addition of KI as a hole scavenger, only trace conversion was observed (entry 10),

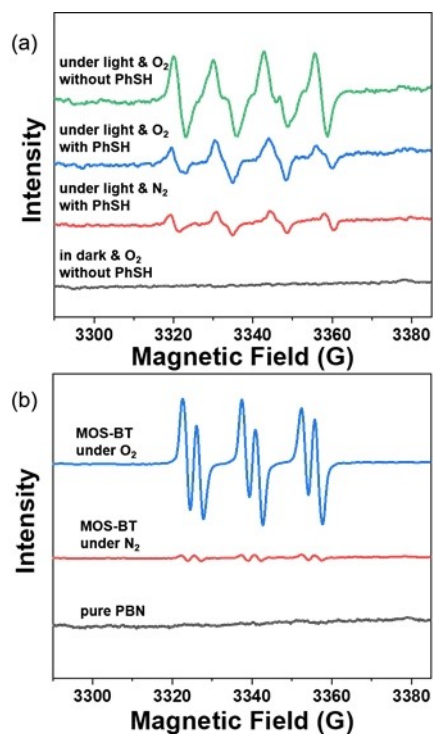**Table 1.** Screening and control experiment of the formation of phenyl aldehyde with diamine as model reaction.[a]

Entry	Catalyst	Reaction condition variations	Conversion [%][b]	Selectivity [%][b]
1[a]	MOS—BT	–	85	97
2	–	no catalyst	trace	0
3	MOS—BT	in dark	trace	0
4	MOS—BT	no thiophenol	trace	0
5	MOS—BT	no O_2, under N_2	12	14
6	MOS—BT	in acetonitrile	20	17
7	MOS—BT	in DMF	60	41
8	MOS—BT	in toluene	63	57
9[c]	MOS—BT	electron scavenger	trace	0
10[d]	MOS—BT	hole scavenger	40	39
11[e]	BTPh$_2$	homogeneous system	>99	95

[a] Standard reaction conditions: [benzaldehyde] = 0.1 M, [1,2-diaminoethane] = 0.3 M, [thiophenol] = 0.1 M, [MOS—BT] = 1 mg/mL, 3 mL DMSO, blue LED lamp (460 nm, 0.26 W/cm^2), room temperature, oxygen, 12 h. [b] Conversion and selectivity determined by GC-MS. [c] Benzoquinone as electron scavenger. [d] KI as hole scavenger. [e] [BTPh$_2$] = 2.8 mM, 12 h.
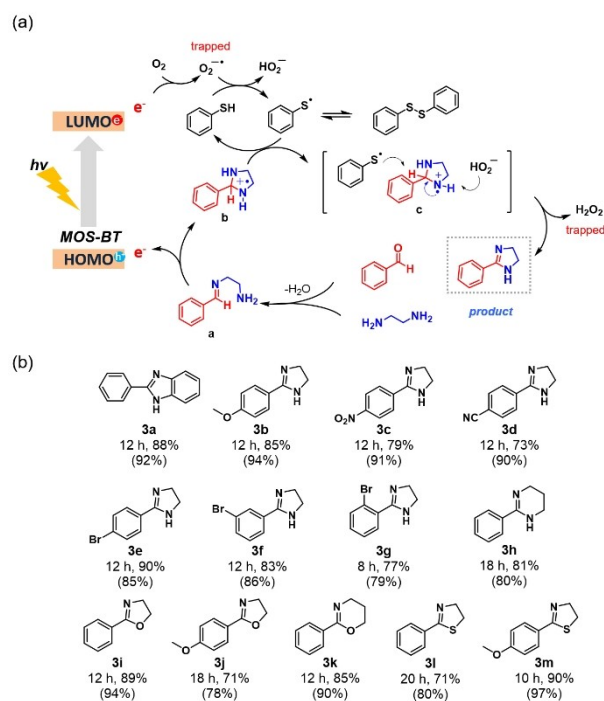

Figure 2. (a) EPR spectra of DMPO—$O_2^{\bullet-}$ adducts with MOS—BT in DMSO as photocatalyst in darkness, under blue light irradiation ($\lambda = 460$ nm, 1.2 W/cm^2) with thiophenol (PhSH) or without thiophenol. (b) EPR spectra using PBN as a radical trapping agent for the radical intermediate of thiophenol under light irradiation. Pure PBN (black), PBN and MOS—BT under N_2 atmosphere (red), under O_2 (blue).

indicating the essential role of holes for the formation of product. The result indicates that the electron-activated superoxide radical ($O_2^{\bullet-}$) could accelerate the addition process as active species. Notably, the catalytic efficiency and selectivity of MOS—BT was comparable with the homogeneous system using BTPh$_2$ (entry 11).

Electron paramagnetic resonance (EPR) experiments were then conducted to precisely study the role of superoxide radical during the reaction. As displayed in Figure 2a, an additional controlling experiment, which implemented the 5,5-dimethyl-1-pyrroline N-oxide (DMPO) as a superoxide radical trapping agent, had appealed typical EPR patterns for DMPO—$O_2^{\bullet-}$ adducts.

Based on the observations, a possible mechanism for obtaining 2-phenyl-2-imidazoline by visible light assisted catalysis is described in Figure 3. First, 1,2-diaminoethane and benzaldehyde are dehydrated and condensed to form imine intermediate **a**. Under visible-light irradiation, intermediate **a** was oxidized by the photogenerated hole of MOS—BT and intramolecular cyclization to form its cationic radical intermediate **b**. Meanwhile, the activated superoxide obtained a hydrogen atom from thiophenol. The intermediate **b** donates one hydrogen atom to thiophenol radical and result in formation of intermediate **c**. Finally, the desired product 2-phenyl-2-imidazoline is produced by deprotonation of **c** by hydrogen abstraction with hydrogen peroxide (Figure S8 in SI). A practical proof of the formation of the radical intermediates could be observed using N-tert-butyl-α-phenylnitrone (PBN) and DMPO as a radical trapping agent (Figure 2). Thiophenol is oxidized by $O_2^{\bullet-}$ during the reaction, the signal of DMPO—$O_2^{\bullet-}$ in the sample added with thiophenol is weaker than that of the sample without thiophenol (Figure 2a). While by adding PBN, the formation of the thiophenol radical could be further observed and a typical

Figure 3. (a) Proposed reaction mechanisms for the photocatalytic formation of 2-phenyl-2-imidazoline. (b) scope of the reactions using MOS—BT as photocatalyst; the value shown in parentheses indicates the selectivity of product.

pattern of PBN trapped radical was logged. Under oxygen atmosphere, the enhanced signal intensity indicated an essential role that oxygen played within the photocatalytic cycle. (Figure 2b).

To further explore the universal feasibility of MOS—BT as photocatalyst, various benzaldehydes and amine derivatives were tested for the azoline formation reaction. As displayed in Figure 3b, high conversion and selectivity were achieved in most examples. Both electron-donating substitution groups on the aryl rings of the substrates (for example methoxy) and electron-withdrawing substitution groups (for example nitro or halides) did not affect the conversion and selectivity. Moreover, the repeating experiments showed that MOS—BT could be reused for the azoline formation reaction for several cycles maintaining a stable level of conversion and selectivity (Figure S9 in SI). The optical properties of MOS—BT barely changed after the recycling experiments, demonstrating its robust nature and reusability as heterogeneous photocatalyst (Figure S10 in SI).

In summary, we designed organosilica containing 4,7-diphenylbenzothiadiazole as efficient heterogeneous and reusable photocatalyst for the formation of N-heterocyclic compounds. The mesoporous organosilica possessed a pore size of ca. 5.7 nm. addition of aromatic aldehydes with various amines can be efficiently catalyzed, forming 2-phenyl-2-imidazoline, 2-phenyl-2-oxazolines, 2-phenyl-2-thiazolines and their derivatives with high conversion and selectivity. This study showed that mesoporous organosilica can be used as efficient photocatalyst with potential for a broader range of photocatalytic reactions.

Acknowledgements

Conflict of Interest

The authors declare no conflict of interest.

[1] a) R. DeSimone, K. Currie, S. Mitchell, J. Darrow, D. Pippin, *Comb. Chem. High Throughput Screening* **2004**, *7*, 473–493; b) L. Kollár, G. Keglevich, *Chem. Rev.* **2010**, *110*, 4257–4302.

[2] a) B. Pfeiffer, K. Hauenstein, P. Merz, J. Gertsch, K.-H. Altmann, *Bioorg. Med. Chem. Lett.* **2009**, *19*, 3760–3763; b) R. S. Roy, A. M. Gehring, J. C. Milne, P. J. Belshaw, C. T. Walsh, *Nat. Prod. Rep.* **1999**, *16*, 249–263.

[3] a) X. Fernandez, R. Fellous, E. Duñach, *Tetrahedron Lett.* **2000**, *41*, 3381–3384; b) K. Sun, D. Li, G. Lu, C. Cai, *ChemCatChem* **2020**.

[4] a) L. Wang, B. Guo, H. X. Li, Q. Li, H. Y. Li, J. P. Lang, *Dalton Trans.* **2013**, *42*, 15570–15580; b) A. Sakakura, R. Kondo, K. Ishihara, *Org. Lett.* **2005**, *7*, 1971–1974; c) I. Mohammadpoor-Baltork, M. Moghadam, S. Tangestaninejad, V. Mirkhani, S. F. Hojati, *Catal. Commun.* **2008**, *9*, 1153–1161.

[5] a) P. Anitha, P. Viswanathamurthi, D. Kesavan, R. J. Butcher, *J. Coord. Chem.* **2015**, *68*, 321–334; b) M. Hosseini-Sarvari, F. Khanivar, F. Moeini, *J. Mater. Sci.* **2015**, *50*, 3065–3074.

[6] Z. Li, H. Song, R. Guo, M. Zuo, C. Hou, S. Sun, X. He, Z. Sun, W. Chu, *Green Chem.* **2019**, *21*, 3602–3605.

[7] a) W. Huang, B. C. Ma, H. Lu, R. Li, L. Wang, K. Landfester, K. A. Zhang, *ACS Catal.* **2017**, *7*, 5438–5442; b) Z. Z. Gao, Z. K. Wang, L. Wei, G. Q. Yin, J. Tian, C. Z. Liu, H. Wang, D. W. Zhang, Y. B. Zhang, X. P. Li, *ACS Appl. Mater. Interfaces* **2019**, *12*, 1404–1411; c) J. Wang, S. Zhuang, *Coord. Chem. Rev.* **2019**, *400*, 213046.

[8] a) X. Wang, S. Blechert, M. Antonietti, *ACS Catal.* **2012**, *2*, 1596–1606; b) Y. Wu, J. Ward-Bond, D. Li, S. Zhang, J. Shi, Z. Jiang, *ACS Catal.* **2018**, *8*, 5664–5674.

[9] R. Li, B. C. Ma, W. Huang, L. Wang, D. Wang, H. Lu, K. Landfester, K. A. Zhang, *ACS Catal.* **2017**, *7*, 3097–3101.

[10] G. Zhang, G. Li, T. Heil, S. Zafeiratos, F. Lai, A. Savateev, M. Antonietti, X. Wang, *Angew. Chem. Int. Ed.* **2019**, *58*, 3433–3437; *Angew. Chem.* **2019**, *131*, 3471–3475.

[11] Z. Zhou, Y. Zhang, Y. Shen, S. Liu, Y. Zhang, *Chem. Soc. Rev.* **2018**, *47*, 2298–2321.

[12] R. Qu, W. Zhang, N. Liu, Q. Zhang, Y. Liu, X. Li, Y. Wei, L. Feng, *ACS Sustainable Chem. Eng.* **2018**, *6*, 8019–8028.

[13] X. Guan, F. Chen, Q. Fang, S. Qiu, *Chem. Soc. Rev.* **2020**, *49*, 1357–1384.

[14] M. Hartmann, A. G. Machoke, W. Schwieger, *Chem. Soc. Rev.* **2016**, *45*, 3313–3330.

[15] a) F. Hoffmann, M. Cornelius, J. Morell, M. Fröba, *Angew. Chem. Int. Ed.* **2006**, *45*, 3216–3251; *Angew. Chem.* **2006**, *118*, 3290–3328; b) X. Liu, S. Inagaki, J. Gong, *Angew. Chem. Int. Ed.* **2016**, *55*, 14924–14950; *Angew. Chem.* **2016**, *128*, 15146–15174; c) T. Asefa, M. J. MacLachlan, N. Coombs, G. A. Ozin, *Nature* **1999**, *402*, 867–871.

[16] a) W. Huang, Z. J. Wang, B. C. Ma, S. Ghasimi, D. Gehrig, F. Laquai, K. Landfester, K. A. Zhang, *J. Mater. Chem. A* **2016**, *4*, 7555–7559; b) E. D. Koutsouroubi, A. K. Xylouri, G. S. Armatas, *Chem. Commun.* **2015**, *51*, 4481–4484; c) H. Takeda, M. Ohashi, T. Tani, O. Ishitani, S. Inagaki, *Inorg. Chem.* **2010**, *49*, 4554–4559; d) N. Mizoshita, T. Tani, S. Inagaki, *Chem. Soc. Rev.* **2011**, *40*, 789–800; e) P. Van Der Voort, D. Esquivel, E. De Canck, F. Goethals, I. Van Driessche, F. J. Romero-Salguero, *Chem. Soc. Rev.* **2013**, *42*, 3913–3955.

[17] a) T. Selvam, A. Machoke, W. Schwieger, *Appl. Catal. A* **2012**, *445*, 92–101; b) J. G. Croissant, X. Cattoen, J. O. Durand, M. W. C. Man, N. M. Khashab, *Nanoscale* **2016**, *8*, 19945–19972.

[18] X. Qian, K. Fuku, Y. Kuwahara, T. Kamegawa, K. Mori, H. Yamashita, *ChemSusChem* **2014**, *7*, 1495–1495.

[19] a) F. S. Mancilha, B. A. DaSilveira Neto, A. S. Lopes, P. F. Moreira Jr, F. H. Quina, R. S. Gonçalves, J. Dupont, *Eur. J. Org. Chem.* **2006**, *2006*, 4924–4933; b) D. Aldakov, M. A. Palacios, P. Anzenbacher, *Chem. Mater.* **2005**, *17*, 5238–5241.

[20] M. S. Lowry, J. I. Goldsmith, J. D. Slinker, R. Rohl, R. A. Pascal, G. G. Malliaras, S. Bernhard, *Chem. Mater.* **2005**, *17*, 5712–5719.